Agricultural Water Management 275 (2023) 108042

Contents lists available at ScienceDirect

Agricultural Water Management

journal homepage: www.elsevier.com/locate/agwat

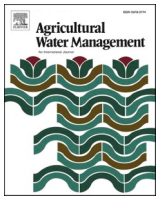

High-resolution 2D modelling for simulating and improving the management of border irrigation

Pierfranco Costabile [a,*], Carmelina Costanzo [a], Fabiola Gangi [b], Carlo Iapige De Gaetani [c], Lorenzo Rossi [c], Claudio Gandolfi [b], Daniele Masseroni [b]

[a] Department of Environmental Engineering, University of Calabria, Via P. Bucci, Cubo 42B, Rende 87036, Italy
[b] Department of Agricultural and Environmental Sciences, University of Milan, Via Celoria 2, Milan, Italy
[c] Department of Civil and Environmental Engineering, Politecnico di Milano, P.zza Leonardo da Vinci 32, Milan, Italy

ARTICLE INFO

Handling Editor - Dr R Thompson

Keywords:
Border irrigation
Two-dimensional modelling
Microtopography
On-field measurements
Operational tools
Irrigation Water Management

ABSTRACT

The structure of an integrated hydrodynamic modelling framework intended to describe the dynamics of surface irrigation is presented in this work. Specifically, the modelling framework, named IrriSurf2D, is constituted by a combination of three elements i.e. (i) high-resolution topographic data of ground surface, (ii) two-dimensional shallow water equations and (iii) one-dimensional Green-Ampt approach for describing infiltration process. The modelling framework was validated with a real case study where timings of waterfront advance and water depths on the field were monitored during a border irrigation event. The results show that IrriSurf2D was able to reproduce both the timings of waterfront advance and the maximum water depths with high accuracy, i.e. with average RMSE below 2 min and 3 cm, respectively. Model performance was robust and accurate even using literature parameters without a tailored calibration of infiltration and roughness parameters. Details of the digital terrain model, which affect the computational grid resolution, had a strong influence on the description of waterfront propagation: a coarse grid resolution (1 m^2) was found inadequate for reproducing reliable timings of waterfront advance and water depths in the field, while with a finer grid (0.01 m^2) as modelling input the simulation results appeared properly consistent with the observations. The modeling approach appears promising to describe the dynamics of border irrigation and paves the way for the development of an operational tool for improving the management of surface irrigation.

1. Introduction

Surface irrigation is the oldest and currently the predominant irrigation practice worldwide (Vico and Porporato, 2011; Soroush et al., 2013; Akbari et al., 2018). According to the information included in the Food and Agriculture Organization's Aquastat Web site (International Commission on Irrigation and Drainage, available at http://www.icid.org/imp_data.pdf - accessed on May 2022) surface irrigation is used on 97% of the irrigated land in India (approx. 60.8 Mha), 94% in China (approx. 57.8 Mha), 44% in the United States (approx. 22.4 Mha) and 100% in Pakistan (approx. 19.6 Mha). In the EU this irrigation practice is predominant in the Padana Plain (i.e. the largest irrigated plain in the EU with about 4.7 Mha of irrigated areas) where irrigated areas are largely watered with surface irrigation methods (Masseroni et al., 2017).

In general, among the different types of surface irrigation, border irrigation is the most common method for watering row crops across the world (Fadul et al., 2020). Despite this irrigation technique continues to interest researchers owing to its low operation and maintenance costs (e.g., very low energy consumptions compared with pressurized systems), border irrigation often suffers from high inefficiency due to over-irrigation and poor application uniformity (Gillies and Smith, 2015; Morris et al., 2015; Chari et al., 2019). In the border irrigation method, water flows down the slope exploiting only gravity and, when the desired amount of water has been delivered to the field, the stream is turned off and this may occur before the water has reached the whole extent of the field. Guidelines defining how to calculate cutoff time according to soil characteristic can be found in literature (Brouwer et al., 1988), even though they should be intended as merely indicative and this decision is typically taken according to the farmer's experience.

In addition, the farmer's experience guides the land preparation before the irrigation season, especially in terms of slope and strip width. Masseroni et al. (2022) found that the correct implementation of these

* Corresponding author.
E-mail address: pierfranco.costabile@unical.it (P. Costabile).

https://doi.org/10.1016/j.agwat.2022.108042
Received 12 August 2022; Received in revised form 31 October 2022; Accepted 8 November 2022
Available online 22 November 2022

"geometrical variables" plays a fundamental role for increasing the efficiency of water usage of border irrigation practice. It follows that, efficient border irrigation systems require proper design and management which can be addressed by using specialized modeling tools (Alavi et al., 2022).

The performance of border irrigation systems depends on border dimensions, border slope, inflow rate, cutoff time, Manning's roughness coefficient and soil infiltration properties (Pereira et al., 2002; Mailapalli, 2008; Smith et al., 2018; Xu et al., 2019). The optimization of irrigation parameters has been an important topic of long-term studies (Smith et al., 2005; Zerihun et al., 1997). Researchers have worked to improve border irrigation performance, mainly optimizing border dimensions (Chen et al., 2013; Anwar et al., 2016), inflow rates, and cutoff times (Morris et al., 2015; Salahou et al., 2018). Evaluating the performance of this irrigation technique can play an essential role in the decisions made by farmers to reduce the gap between the potential and actual performance, increasing water use efficiency at the field scale. The first step to achieve this is to evaluate the current performance of border irrigation events. For this purpose, first, the hydraulic behavior of the waterfront advancement should be described by hydrodynamic models, and the models should be calibrated and validated by observed data (Sharifi et al., 2021). Secondly, the simulations obtained changing geometrical (border slope, border width, border length etc.) and/or kinematic variables (inflow rate, irrigation duration, etc.) in the calibrated hydrodynamic models should suggest novel design and management strategies based on the optimization of irrigation performances in terms of application efficiency and distribution uniformity (Mazarei et al., 2020).

A wide range of numerical models has been proposed to simulate border irrigation systems. Changes have been relevant from the standpoint of the equations on which these models were based. Researchers started solving simplified versions of the one-dimensional Saint–Venant equations, i.e., kinematic-wave (e.g., Walker and Humpherys, 1983) and diffusion-wave (e.g., Clemmens, 1979; Strelkoff and Souza, 1984; Schmitz and Seus, 1989) approximations. One-dimensional (1D) field scale models such as WinSRFR (Bautista et al., 2009), SIRMOD (Walker, 2003) and SISCO (Gillies and Smith, 2015) are commonly used to simulate border irrigation. These models assume that the waterfront is uniform along the border width and they cannot examine the impacts on irrigation performances of engineered changes in the field microtopography. In such circumstances, two-dimensional models should be used when the variations of both longitudinal and transverse components of the waterfront are significant, such as water flow velocity and water depth (Strelkoff et al., 2003). Two-dimensional simulations permit overcoming many problems related to one-dimensional modeling. Among them, there are irregular field geometries or the spatial variability of key irrigation variables. Khanna and Malano (2006) reviewed several surface irrigation models in the literature. They concluded that two-dimensional models had higher capabilities than one-dimensional models. Furthermore, these authors reported that the inclusion of microtopography (soil undulations) could improve the accuracy of simulations. Moreover, many borders are characterized by irregular layouts (Singh and Bhallamudi, 1997; Khanna et al., 2003), or are irrigated by several point inflows. These situations are best simulated with two-dimensional models.

Surface water flow in border irrigation is shallow and can be accurately described by complete hydrodynamic equations (also called Shallow Water Equations - SWE). In two-dimensional problems, Playán et al. (1994, 1996) proposed a numerical model for surface water flows in border irrigation based on the finite-difference approach. Singh and Bhallamudi (1997), Bradford and Katopodes (2001), and Brufau et al. (2002) developed numerical models by using the finite-volume approach. Gandolfi and Savi (2000) developed a mathematical model which integrates the complete two-dimensional SWEs with the one-dimensional Richards' equations.

To reduce the computational time and the complexity of the numerical schemes, some approaches based on simplified governing equations have been proposed, considering that surface water flow in border irrigation is slow. Thus, inertia terms (or acceleration terms) of the complete hydrodynamic equations are sometimes ignored, and zero-inertia equations have been proposed. These equations can be solved by a numerical approach more easily than complete hydrodynamic equations because of their simple mathematical properties (Strelkoff et al., 2003; Zhang et al., 2017). In this context, Liu et al. (2020) validated a zero-inertia model even in presence of rapidly varied inflow discharge.

Naghedifar et al. (2019) proposed a basin/border irrigation model combining the 2D overland flow equations, based on the diffusion-wave approximation of the SWEs, with the 3D infiltration computed by the mixed form of Richards' equation using a non-orthogonal curvilinear coordinate system to speed-up the model computation performance. Liu et al. (2021) developed a semi-Lagrangian solution of the 2D shallow water equations that was found to be, computationally, six times more efficient than the Eulerian scheme considered by the authors. Githui et al. (2020) adapted the 2D ANUGA model, originally developed for inundation simulations, to simulate border and basin irrigation by incorporating an infiltration algorithm based on empirical formulations.

The correct implementation of the infiltration process is an important work that can help to improve the description of the dynamics of border irrigations (Bautista et al., 2009). From a physical point of view, most of the water applied during irrigation events infilters in the vertical direction, whereas later infiltration through the berms can be ignored (Bo et al., 2012). According to this, traditional tools such as WinSRFR, SIRMOD and SISCO, use one-dimensional empirical formulas for infiltration computations, where all variables are functions of distance and time, only. The most widely applied family of infiltration formulations is the one based on Kostiakov equations (Kostiakov, 1932), which models a declining infiltration rate with the opportunity time (i.e. the time during which water is available for infiltration at each point along the length of the wetted border). A modification of the Kostiakov equation for taking into account the macropore infiltration was proposed by Lewis (1937) and this new formulation is well known in the literature as Kostiakov-Lewis equation. Despite Kostiakov equation have a long history of use in surface irrigation engineering analyses, they require to be well-calibrated to fit accurately the real infiltration processes. Therefore, measures of advance and recession trajectories or of the volumetric water content at different depths and along the longitudinal direction of the field should be performed at each irrigation event for a good determination of infiltration parameters (Pereira et al., 2007). More complex physical formulations, such as Richards' equation, were tested and implemented in two-dimensional hydrodynamic models (Gandolfi and Savi, 2000) but difficulties to reach converged solutions in reasonable computational times were observed. The semi-physical approaches appear to be the better solutions (Kacimov et al., 2010), since they reproduce a simplistic but elegant approximation for infiltration when water is ponded on the soil surface.

In light of the previous considerations, this work proposes a novel integrated modelling framework based on the combination of on-field measurements and hydrodynamic modelling for describing the dynamics of border irrigation. More in detail, in this work the structure of the modelling framework is constituted by a combination of (i) high-resolution topographic information and (ii) two-dimensional surface hydrodynamic modelling coupled with a semi-physical infiltration modelling that will be described and tested. The proposed approach overcomes the simplification related to (i) the one-dimensional water front advance description, (ii) the empirical representation of the infiltration processes, (iii) the flat delineation of the ground surface, providing a tool that might support the management of border irrigations at field scale. Performances of the proposed approach, evaluated in terms of the ability to describe (i) the times of the waterfront advance and (ii) the actual water depths along the longitudinal direction of the field during irrigations, have been estimated by comparing modelling outputs with observations obtained in a real-world case study where

border irrigation events were accurately monitored during the 2022 agricultural season.

2. Framework of the modelling approach

Correct management of the water distribution onto the field during the irrigation events can help to reduce water consumption, making the watering more consistent with the crop water needs. To reach this goal in the context of border irrigations, an optimal combination of flow rate, cutoff time/distance, field/strip size and slope should be investigated. The proposed modelling framework, whose structure is reported in Fig. 1, provides a useful tool able to analyze the impact of different combinations of these variables on the overall performance of border irrigations. It combines microtopography, infiltration and hydrodynamic information and takes advantage of direct on-field measurements (when available) for improving the description of surface water dynamics on borders. In the following, the main components of the modelling framework are presented.

2.1. Exploring microtopographic characteristics of the ground surface

Several studies emphasized the need to pay more attention to the spatial variability of microtopography in basin irrigation design for management and decision-making purposes (see for example Bai et al., 2017; Bai et al., 2011). Moreover, there is some evidence that the spatial variability of surface elevations has more influence on basin irrigation performance than the spatial variability of infiltration (Zapata and Playán, 2000). On the other hand, the potential of the 2D fully-dynamic shallow water modelling for the management of surface irrigation systems can be effectively explored once high-resolution topographic surface models are available, to finely describe the physical effects associated to the inertial and convective terms that gain more significance in high resolution modeling, especially in the case of low water depths (Cea and Costabile, 2022). To this aim, several survey techniques are available and the use of Uncrewed Aerial Vehicles (UAV) for performing photogrammetric surveys fits very well in this context. In fact, by properly setting flight parameters (see, e.g., Pagliari et al., 2017) Ground Sample Distance (GSD), i.e. the average ground resolution of the digital acquisitions, of centimeter level can be reached. Moreover, measuring also some Ground Control Points (GCPs) by GNSS or Total Stations (Gagliolo et al., 2018) accuracies at the same level of GSD can be obtained. This means that the photogrammetric-derived Digital Terrain Models (DTMs) meet the requirements of microtopography.

2.2. Describing water propagation onto the field

Simulation of the water propagation on the border strips has been based on the fully dynamic version of the 2D Shallow Water Equations, expressed in Eq. (1):

$$\frac{\partial \mathbf{U}}{\partial t}+\frac{\partial \mathbf{F}}{\partial x}+\frac{\partial \mathbf{G}}{\partial y}=\mathbf{S} \tag{1}$$

where:

$$\mathbf{U}=\begin{pmatrix} h \\ hu \\ hv \end{pmatrix};\ \mathbf{F}=\begin{pmatrix} hu \\ hu^2+\frac{gh^2}{2} \\ huv \end{pmatrix};\ \mathbf{G}=\begin{pmatrix} hv \\ huv \\ hv^2+\frac{gh^2}{2} \end{pmatrix};\ \mathbf{S}=\begin{pmatrix} r-f \\ gh\left(S_{0,x}-S_{f,x}\right) \\ gh\left(S_{0,y}-S_{f,y}\right) \end{pmatrix} \tag{2}$$

in which: t (s) is time; x (m) and y (m) are the horizontal coordinates; h (m) is the water depth; u (m/s), v (m/s) are the depth-averaged flow velocities in x- and y- directions; g (m/s^2) is the gravitational acceleration; f (m/s) is the infiltration losses; $S_{0,x}$ (m/m) and $S_{0,y}$ (m/m) are the bed slopes in x- and y- directions; $S_{f,x}$ (m/m) and $S_{f,y}$ (m/m) are the friction slopes in x- and y- directions. $S_{f,x}$ and $S_{f,y}$ were computed as in Eq. (3):

$$S_{f,x}=\frac{n^2u\sqrt{u^2+v^2}}{h^{4/3}},\ S_{f,y}=\frac{n^2v\sqrt{u^2+v^2}}{h^{4/3}} \tag{3}$$

in which n is the Manning coefficient, which is one of the parameters of the model that needs calibration.

The numerical integration of Eq. (1) was obtained using the IrriSurf2D code, which is a specific extension for border irrigation of the

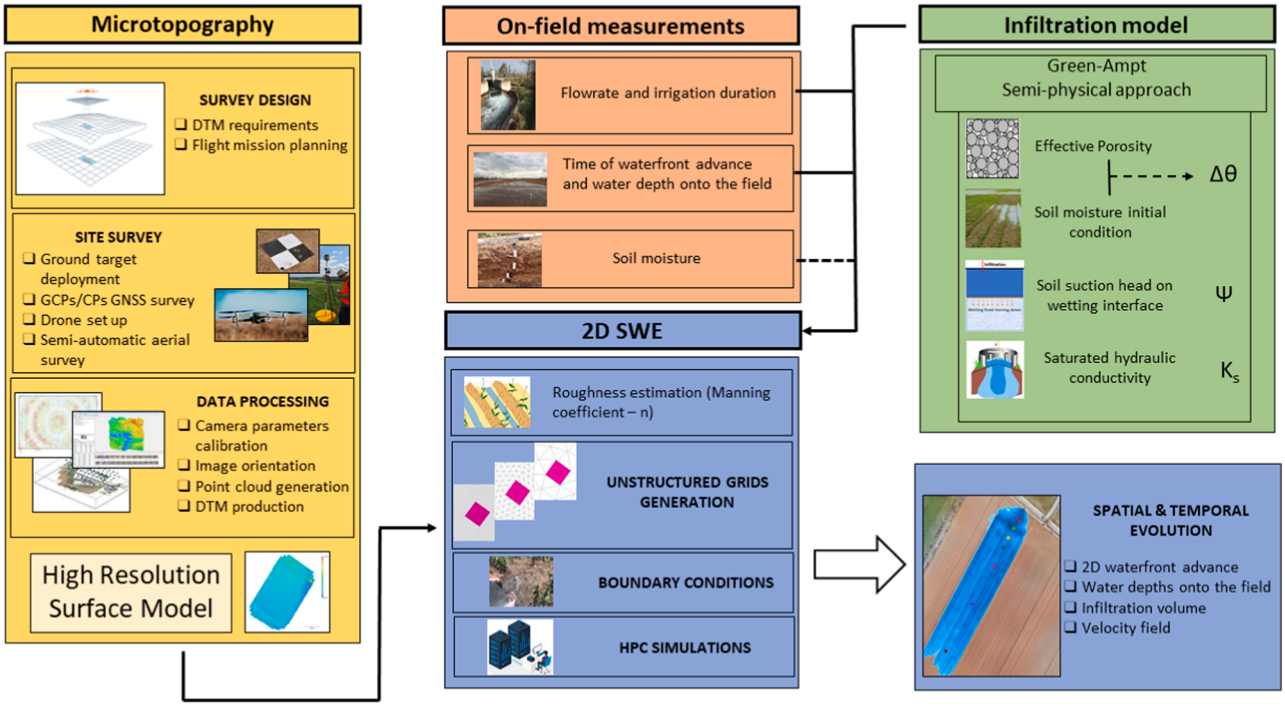

Fig. 1. Methodology workflow.

flood propagation model, developed for research purposes at the University of Calabria (Italy), based on the expertise in the field of fluvial, pluvial and urban flood modelling acquired in previous studies (among the most recent ones see, for example, Costabile et al., 2020; Costabile and Costanzo, 2021; Costabile et al., 2021; Padulano et al., 2021; Costabile et al., 2022; Barbero et al., 2022). The key features of IrriSurf2D include the use of the well-known Roe Riemann solver for the computation of the numerical fluxes, the adoption of an upwind approach to discretize the bottom variations and of a semi-implicit treatment of the friction source term. Finally, the time steps are estimated according to the Courant-Friedrichs-Lewy condition to ensure the model stability, the computational domain is generated using an unstructured grid of irregular triangular elements and a robust wet-dry procedure is considered.

IrriSurf2D is coded in Fortran 90 and is configured for parallel execution using Message Passing Interface (MPI) directives in order to reduce computational time.

2.3. Simulating infiltration process

The infiltration process in the IrriSurf2D model has been simulated through the semi-physical Green-Ampt (GA) formula (Green and Ampt, 1911) described by Eq. (4).

$$F(t) = K_s t + \psi \Delta\theta \ln\left(1 + \frac{F(t)}{\psi \Delta\theta}\right) \tag{4}$$

where F represents the cumulative amount of infiltrated water, K_s is the conductivity of the saturated profile, $\Delta\theta$ is the difference between the water content of the saturated soil (approx. the soil effective porosity - η), and the initial water content (ϑ_i) before infiltration began, ψ is the soil suction head on the interface between the wet soil layer and the underlining dry soil. The GA formula has been chosen due to (*i*) the simplicity in its implementation and computation and (*ii*) the definition of its parameters which have a physical meaning. Therefore, they can be adjusted within realistic ranges of values obtained from previous literature experiences achieved in similar contexts of the examined fields. The infiltration losses f in Eq. (5) have been then evaluated by deriving Eq. (4) over time:

$$f(t) = K_s + \frac{K\psi\Delta\theta}{F(t)} \tag{5}$$

The discretization in time of Eqs. (4) and (5) and the valuation of the rate of water available to infiltrate, before and after the ponding time, are calculated in a coupled manner within the SWEs considering the approach proposed in Fiedler and Ramirez (2000).

3. Application of the modelling framework on a real-world case study

3.1. Field characteristics

The performances of the modelling approach were evaluated by comparing the simulated and observed timings of the waterfront advance and water depths along the field monitored during one of the watering events carried out in a maize field (about 2 ha in size and subdivided into strip sectors) located in the Padana Plain (i.e. the largest irrigated plain in EU) in the year 2022. The employed irrigation method in the experimental field is closed border irrigation. More in detail, the water flows onto the field through a series of steel gates which are opened manually in sequence to supply water to each strip, starting from the main supply canal at the upper end of the field. This practice is shown in Fig. 2, where the first watering carried out in the experimental field immediately after the sowing in the year 2021 is presented.

Once the water is released onto the field, it is gravity-driven following the longitudinal slope of the field. This latter was found at about 6.5‰ through the procedure described in Section 3.2.1. The monitored irrigation event was performed on May 23, about one month after the sowing. With regards to soil properties, disturbed soil samples at different depths (about 10, 30 and 50 cm) were collected at five different points of the field to evaluate soil texture. The analysis of the samples showed a predominance of sandy, sandy-loam texture with a skeleton higher than 30%. No vertical pattern in soil layers was found in the field, which could thus be considered homogeneous along the vertical profile. The level of the groundwater table was about 5 m from the ground surface, thus the potential interactions of the capillary fringe with the infiltration process can be neglected. Additional information about the study domain is reported by Masseroni et al. (2022), whereas specific information regarding the monitored field is summarized in Table 1.

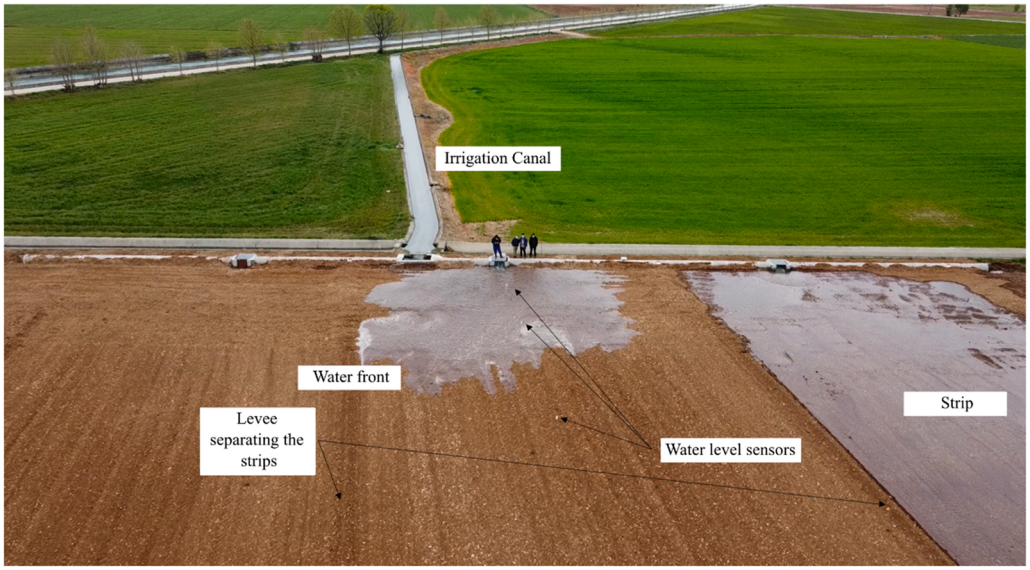

Fig. 2. Border strip irrigation performed onto the experimental field immediately after the sowing in the year 2021. Rearranged by Masseroni et al. (2022).

Table 1
Details on the characteristics of the experimental field.

Characteristics	Value
Coordinates (WGS84-Lon,Lat)	(10.6873,45.3025)
Size (ha)	1.7
Number of strips	5
Average strip width (m)	18
Average strip length (m)	188
Average strip slope (‰)	6.5
Crop	Maize
Cultivar	Pioneer P2088 – 70 (FAO 300)
Sowing date	27th March 2022
Harvesting date	1st August 2022
Soil texture*	Sandy/sandy-loam

* According to the United States Department of Agriculture definitions.

3.2. Measurements

3.2.1. Microtopography survey

Microtopography of the ground surface of the experimental field was determined just after the sowing through a photogrammetric flight performed through a DJI Mavic 2 Pro UAV, acquiring 366 images at about 36.5 m a.g.l., leading to a GSD of about 0.8 cm. The images were processed with the Agisoft Metashape software (version 1.7.0), including also some GCPs that were measured by NRTK-GNSS (Network Real Time Kinematic Global Navigation Satellite System) with a centimetric accuracy. The estimated model accuracy evaluated at the GCPs is 1.0 cm and 2.5 cm in the planimetric and altimetric components, respectively. From the photogrammetric dense point cloud a Digital Terrain Model (DTM) with about 3 cm resolution was computed and provided as input of the two-dimensional hydrodynamic modelling. The DTM of the experimental field is shown in Fig. 3.

3.2.2. Flow rate and irrigation event duration

The flow rate during the irrigation event was determined by measuring the flow level in the supply canals, where the flow can reasonably be considered to be in uniform condition. The roughness parameter was calibrated at the beginning of the irrigation season, using the well-known Manning-Strickler formula (Ven Te Chow, 1959) in which: 1) the flow rate was measured by a manual portable magnetic-inductive flow meter (Flow Sensor NAUTILUS C 2000, OTT, USA) by using the so-called conventional current meter methodology (Anon, 2010; Peruzzi et al., 2021), 2) the canal slope was evaluated using a portable Global Positioning System (GPS) (GRS-1, TOPCON, Japan – vertical accuracy of ± 2.5 cm), 3) the cross-section area and the hydraulic radius were computed considering the shape of the cross-section (trapezoidal) and a graduated rod (precision is ± 1 mm) for the measurement of the water depth. Using this information, the

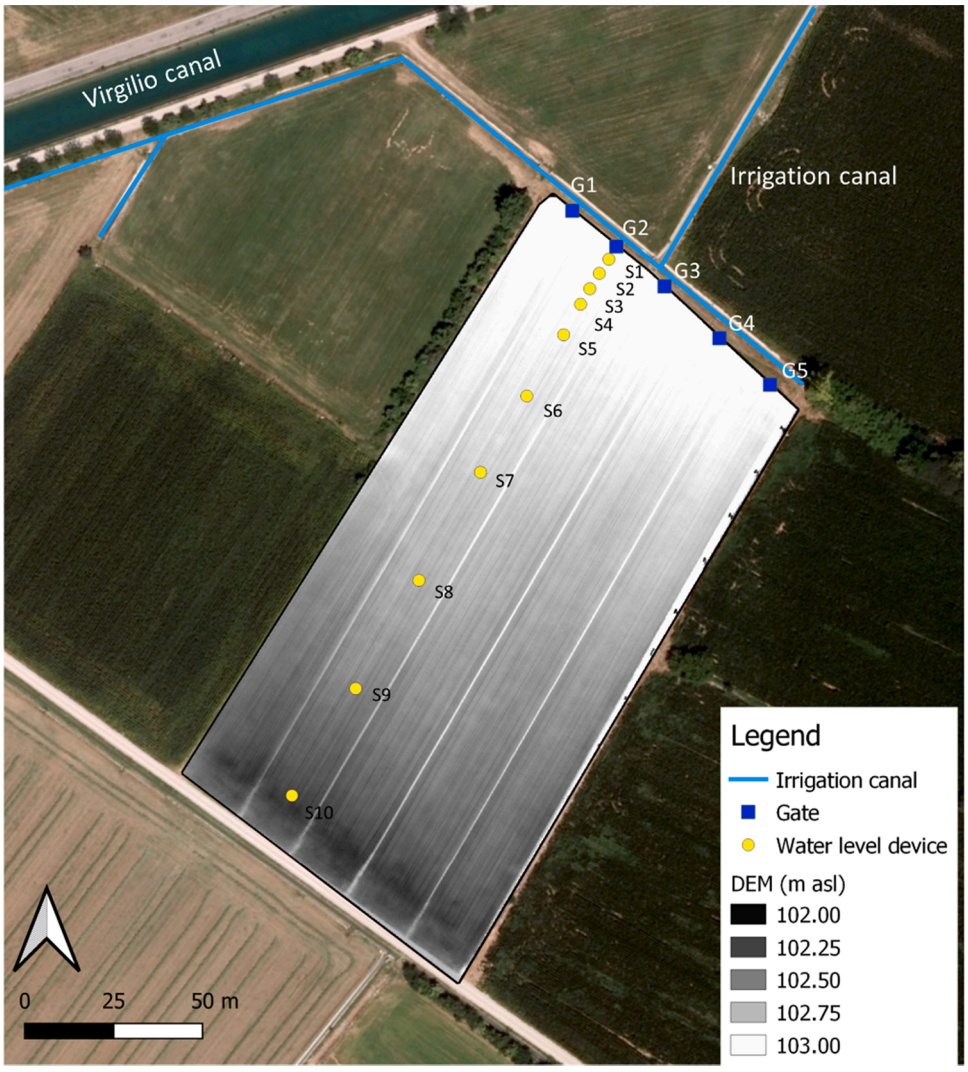

Fig. 3. Digital Terrain Model of the experimental field. The arrangement of the strips is also visible. Irrigation channels are represented by light blue lines, irrigation inlet gates for each strip by blue dots, and the position of the ten water level sensors (S1,S2,..., S10) by yellow dots.

estimated Strickler coefficient was equal to 75 $m^{1/3}$ s^{-1}. The watering time of each strip of the experimental field was measured using a chronometer during the irrigation event. Additional information on the measurement campaigns is reported in Masseroni et al. (2022).

3.2.3. Water depth onto the field

The monitoring of the water depth evolution onto the field during the irrigation event, and therefore the timings of the waterfront advance, was carried out through 10 crafted water level devices (specifically developed for this study), which were installed along the longitudinal direction of the field (see S1, S2..., S10 shown in Fig. 3). Such devices consist of an Arduino Nano® microcontroller and they are equipped with an ultrasonic range finder sensor HY-SRF 05 model (Az-Delivery, Germany). The single sensor works as both an ultrasound transmitter and receiver and it can be used to measure distances in a range between 0.02 and 4.5 m with resolution up to 0.2 cm, a maximum measurement frequency of 40 Hz and a detection angle of 15°. A digital thermometer DS18B20 model (Az-Delivery, Germany) was used to adjust the ultrasonic signal on the basis of air temperature. Distance data were recorded every 0.2 s and downloaded insitu at the end of the irrigation intervention. The device was able to detect distances under different flow regimes with a high level of accuracy, as demonstrated during several tests performed in the open-channel flume of the hydraulic laboratory of the University of Pavia, Italy. Fig. 4 shows the electronic circuit diagram of the water level device and an example of its installation in the field. The sensors were installed in the second sector just before the irrigation event and removed right after the water depth across the field was completely depleted. The water level sensors were installed at 5, 10, 15, 20, 30, 50, 75, 110, 145 and 180 m from the head of the field (see Fig. 3).

3.3. Modelling settings

The model setup can be summarized as follows: 1) generation of the computational grid for a required spatial resolution, 2) determination of the initial and boundary conditions, 3) parameters assumptions and estimations.

As mentioned in Section 2.2, the numerical model is built upon computational domains represented by irregular triangular elements, so that a variable resolution can be set throughout the field. However, the use of a uniform resolution is more practical considering the purposes of the work. Specifically, we generated three different grids having substantially uniform resolutions: 0.01 m^2 (fine grid), 0.1 m^2 (medium grid) and 1 m^2 (coarse grid), in order to assess how much the dynamics of surface irrigation are influenced by the microtopographic features of the field. The numerical grids were generated using the Aquaveo™- SMS (Surface-water Modeling System) software in which it was possible to interpolate the ground levels, related to the input DTM described in Section 3.2.1, onto the grid nodes associated with the fine, medium and coarse grid. In practice, the microtopographic features are progressively lost when moving from the fine to the coarse grid, being only the finer grid able to adequately exploit all the topographic information.

As regards the boundary conditions, we imposed the flow rate and the cutoff time of the examined sector in the computational cells that cover the inflow section, and the associated critical flow condition for the computation of the water depths. Downstream, we set closed boundary conditions. The field was assumed to be initially dry, so the water depths were set to a very low value everywhere (10^{-9} m).

Finally, the four parameters of the model (n, K_s, $\Delta\theta$, ψ) were assumed uniformly distributed onto the field. This assumption is reasonable, at least for the parameter related to the GA formula since the soil samples revealed that the soil was quite homogeneous along all directions of the field. The initial soil moisture condition was obtained from a multilevel soil moisture probe (Teros12, Meter, Group, USA) averaging the monitored volumetric water content just before the irrigation event over about 0.5 m of depth (i.e. approximately the depth of the rooted layer). The initial soil moisture ϑ_i was then subtracted from the effective porosity η to obtain $\Delta\theta$, i.e. the actual soil space that water can exploit during the infiltration process.

3.4. Performance evaluation

The performance of the modelling approach was evaluated by comparing observed and simulated times of the waterfront advance and the water depths along the longitudinal direction of the field. The metric used for this purpose was the Root Mean Square Error (RMSE) described in Eq. (6).

$$RMSE = \sqrt{\frac{1}{N} \bullet \sum_{i=1}^{N} (P_i - O_i)^2} \tag{6}$$

Where P_i are the simulated values, O_i are the observed values and N is the total number of observations.

Before evaluating the IrriSurf2D model performance, the four parameters of the model (K_s, ψ, Δθ and n) were calibrated using an expeditious procedure. Considering as border conditions the flow rate and the cutoff time of the examined sector (i.e. the second sector) and as a computational mesh a fine grid resolution of 0.01 m^2, the model parameters were estimated with the aim to reproduce the observed timings

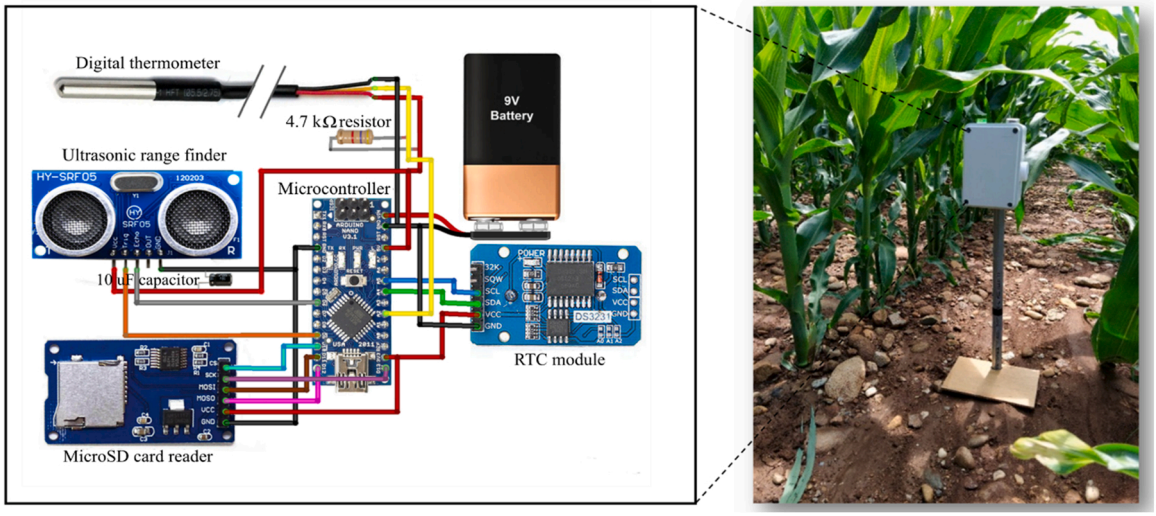

Fig. 4. Electronic circuit and in-field installation of the homemade water level sensors.

of waterfront advance, but ensuring also a reasonable prediction of the maximum water depths along the longitudinal direction of the field. Starting from the ranges typically proposed in literature for both GA parameters in sandy/sandy loam soils and the roughness of cultivated fields (Rawls et al., 1983), the model parameters were slightly adjusted to fit the observed data. The comparison between model results and experimental measurements was analyzed from a statistical point of view. Specifically, in order to filter out the noise component and uncertainty in the DTM generation and, consequently, in the simulation results, the median of the simulated values in an area of 2 m^2 surrounding the position of water level sensors was computed instead of considering the simulated water depth in the computational cell closest to the position of the sensors themselves.

The effects of different grid resolutions on model performances were examined as well, considering the computational grids mentioned in Section 3.3.

4. Results

4.1. Characteristics of the irrigation event

The characteristics of the selected irrigation event are summarized in Table 2, where the flow rate, cutoff time, an average water depth and volume of irrigation are presented for each irrigated sector. The average flow rate and irrigation duration were respectively about 350 l/s and 31 min. The applied water depth and the irrigated volume for the sector resulted in about 180 mm and 650 m^3 on average. Overall, a total volume of irrigation of about 3200 m^3 was distributed onto the field with an irrigation event duration of about 2.5 h. Concerning the examined sector (i.e. the second sector), it was irrigated with a flow rate of 354 l/s for 35 min. This led to an applied water depth onto the sector of about 188 mm. The monitored volumetric soil water content before the irrigation event of May 23rd resulted to be about 0.2 m^3/m^3, i.e. about half of the effective porosity generally indicated in literature for sandy/sandy loam soils ($\eta = 0.4$).

Table 2
Characteristics of the 23rd May irrigation event subdivided for each irrigated sector.

Gate	Flow rate (l/s)	Irrigation duration (min)	Applied water depth (mm)	Volume of irrigation (m^3)
1	349	35	114	419
2	*354*	*35*	*188*	*637*
3	349	37	195	775
4	344	30	191	722
5	338	20	224	721
Average	347	31	182	655
St. Dev.	5.9	6.9	41.1	140.8

4.2. Performance of the modelling approach

The results of the nine simulations performed adjusting the Irri-Surf2D model parameters are summarized in Table 3. More in detail, the model parameters were adjusted starting from the selected literature parameters reported in SIM1 for a sandy-sandy/loam type of soil. In general, all simulations resulted consistent with the observations for both timings of waterfront advance and maximum water depths. The RMSE between the observed and simulated periods of the waterfront advance was less than 7 min in all cases, whereas between observed and simulated maximum water depth was less than 5 cm. The SIM 8, characterized by n, K_s, $\Delta\theta$ and Ψ respectively equal to 0.1 s/$m^{1/3}$, 100 mm/h, 0.2 and 20 cm, has resulted to be the more accurate simulation with an average RMSE (over the ten monitored points) of about 1 min between observed and simulated times of the waterfront advance and 2.7 cm between observed and simulated maximum water depths. Therefore, these parameters were considered in the analysis discussed in the following sections.

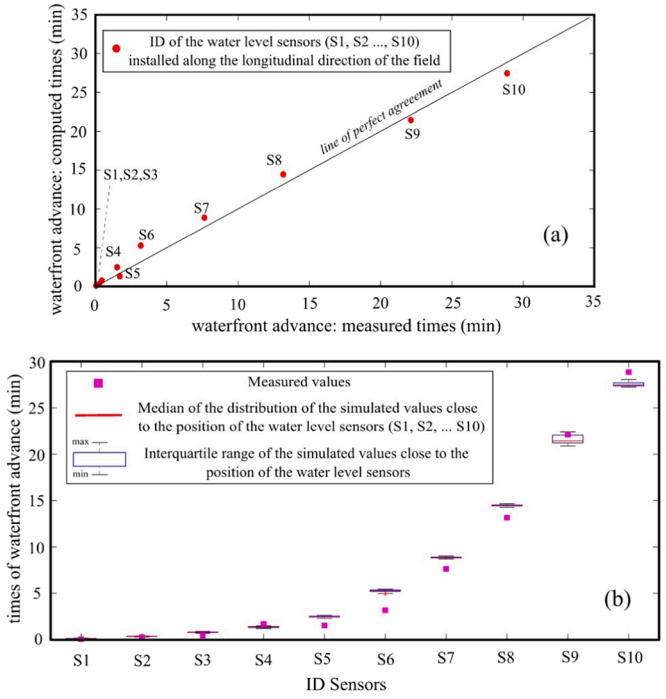

Fig. 5. (a) Comparison between measured and computed (median) times of water advance and (b) box plot related to the statistical evaluation of the results (red lines, blue boxes and black horizontal lines refer, respectively, to the median, the interquartile range and minimum/maximum of the distribution of the simulated values close to the position of the water levels sensors - S1, S2, …, S10 - highlighted in Fig. 3).

Table 3
Model parameters and simulation metrics.

	Model Parameters						Simulation Metrics	
	n s/$m^{1/3}$	Ks mm/h	Ψ cm	η –	ϑ_i –	$\Delta\theta$ –	*RMSE Time of the waterfront advance (min)*	*RMSE Maximum water depth (cm)*
SIM1	*0.1*	*100*	*5*	*0.4*	*0.2*	*0.2*	*1.9*	*3.3*
SIM2	0.1	50	5	0.4	0.2	0.2	2.8	3.8
SIM3	0.1	25	5	0.4	0.2	0.2	3.2	4.1
SIM4	0.1	100	5	0.6	0.2	0.4	1.1	2.8
SIM5	0.1	100	5	0.3	0.2	0.1	2.4	3.5
SIM6	0.05	100	5	0.4	0.2	0.2	5.1	4.5
SIM7	0.2	100	5	0.4	0.2	0.2	6.7	4.2
SIM8	0.1	100	20	0.4	0.2	0.2	1.1	2.7
SIM9	0.1	100	1	0.4	0.2	0.2	2.3	3.4

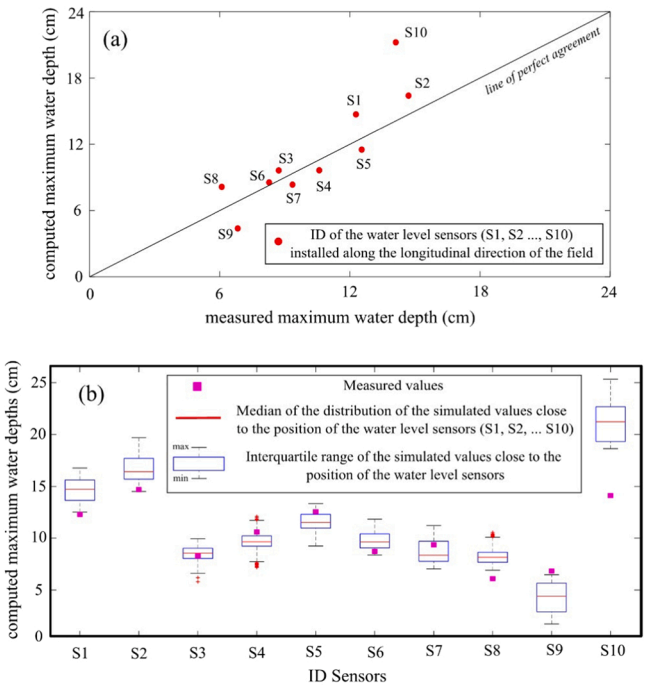

Fig. 6. (a) Comparison between measured and computed (median) maximum water depths and (b) box plot related to the statistical evaluation of the results (red lines, blue boxes and black horizontal lines refer, respectively, to the median, the interquartile range and minimum/maximum of the distribution of the simulated values close to the position of the water levels sensors - S1, S2, …, S10 - highlighted in Fig. 3).

The computational time needed to perform a generic simulation is approximately 30 min for 60 min of the real event. Considering the number of cells (approximately 10^6) and, mostly, the very low value of their size (0.01 m^2) that drastically limits the time step according to the stability requirements provided by the CFL condition, the efficiency of the numerical model can be considered good.

The model performances are also reported in Figs. 5 and 6 where the scatter plot of the computed and observed times of the waterfront advance and maximum water depths is followed by a comparison between simulated and measured values of times of the waterfront advance and maximum water depths along the longitudinal direction of the field. Fig. 5a shows the very good performances of model predictions in terms of times of water advance, since the points are very close to the line of perfect agreement. As further confirmation, the coefficient of determination R^2 is approximately equal to 0.99. A limited variability of model estimations was observed also along the longitudinal direction of the field as shown in Fig. 5b. In general, the interquartile range resulted less than 1 min in all the monitored points.

The accuracies in reproducing the maximum water depths are less than those obtained for the times of water advance but they can be considered acceptable for the purpose of the modelling framework (i.e. supporting the surface irrigation management). Computed and observed maximum water depths resulted slightly dispersed around the line of perfect agreement, as shown in Fig. 6a. In this case, the coefficient of determination R^2 is equal to 0.77. In addition, the variability of model estimation along the longitudinal direction of the field resulted more emphasized at the beginning and at end of the field (point S1, S2, S9 and S10) with an interquartile range of about 2–3 cm, that is more than double, on average, than that obtained between S3 and S8 (Fig. 6b).

The evolution of measured and simulated water depths onto the field is reported in Fig. 7. In general, the model appears able to reliably reproduce the observed water depths in all monitored points (i.e. from S1 to S10). Small differences were observed in the last part of the field where overestimations of the simulated water depths with respect to

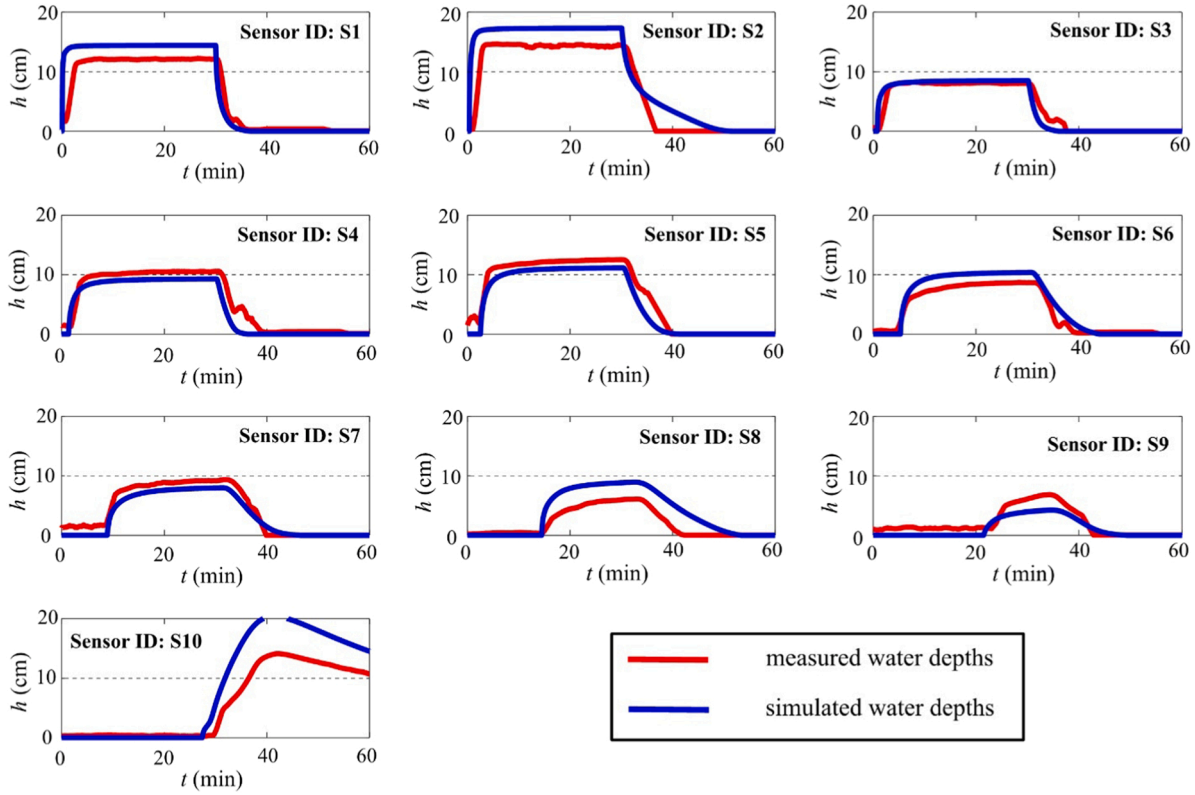

Fig. 7. Comparison between measured and simulated water depths *h* onto the field for each sensor (S1, S2, ..., S10 shown in Fig. 3).

Table 4
Effects of the grid resolution on model performance.

Grid Resolution	RMSE (min) Time of the waterfront advance	RMSE (cm) Maximum water depths
Fine (0.01 m^2)	1.1	2.7
Medium (0.1 m^2)	11.8	5.4
Coarse (1 m^2)	12.5	6.9

measurements were found, probably due to some boundary effect. Simulated shapes of water depletion after irrigation appear very consistent with the observations in all monitored points, confirming the accuracy of the GA approach in the description of the infiltration process in border irrigation.

4.3. Effects of grid resolution on model performance

Medium and coarse grids defined in Section 3.3 were used to perform simulations aimed at the evaluation of the effects on the model performance caused by different resolutions. The results are shown in Table 4 where the RMSE between observed and simulated times of waterfront advance and maximum water depths is reported for the three different considered grid resolutions. In general, a significant reduction in model performances was found when the detail of the computational grid changes from fine to coarse. The RMSE increased by about 12 times on average in case of time of waterfront advance (1.1 min in fine grid and 12.5 min in coarse grid), and by about 2 times in case of maximum water depth (2.7 cm in fine grid and 6.9 cm in coarse grid).

The decreasing of model performance connected with the lowering of grid resolution had repercussions on the description of surface flow dynamics. In Fig. 8, the timings of waterfront advance (Fig. 8a) and the maximum water depths (Fig. 8b) for different grid resolutions are compared. A significant reduction in the speed of waterfront advance was found at a distance of about 50 m from the head of the field (which corresponds with the position of sensor S6) if the coarse grid was considered. In this case, the waterfront advance was interrupted before reaching the end of the field. The same effect was found using in the model a medium grid, but in this case, the waterfront advance was interrupted at about 110 m from the head of the field (i.e. where S8 sensor is located). Using a fine grid, instead, the model was able to match the observations both in case of times of waterfront advance and the maximum water depths.

In Fig. 9 the effects of the changes in grid resolution on the temporal evolution of the waterfront advance are presented. In particular, three instants in time i.e. 1, 5 and 10 min following the irrigation event were considered. The results show that the use of the fine grid allows an accurate and more realistic simulation of the waterfront advance which, instead, is not captured by using the grid with 1 m^2 of resolution. Significant differences in progressive waterfront distances from the head of the field were accumulated during the simulation. In particular, about 25 m of difference in waterfront advance between fine and coarse grid were found after 10 min of simulation. Errors in the lateral spread of waterfront advance were also found if the coarse grid is used. In particular, from 5 min onward unrealistic lateral overflows were reproduced as a consequence of a minor topographic detail that is not able to consider the presence of the levees separating the strips. The differences in grid resolutions affect the spatial distribution of cumulative infiltration volumes as well (Fig. 10). Considering the coarse grid, the infiltration process remained confined to the first 65 m, i.e. about 30% of the total length of the field.

Clearly, the simulations related to the medium and coarse grid are computationally less demanding than that one based on the fine grid. As regards the medium grid (10^5 elements), the computational time was approximately 2 min whereas only 27 s were needed to perform a generic simulation using the coarse grid (10^4 elements).

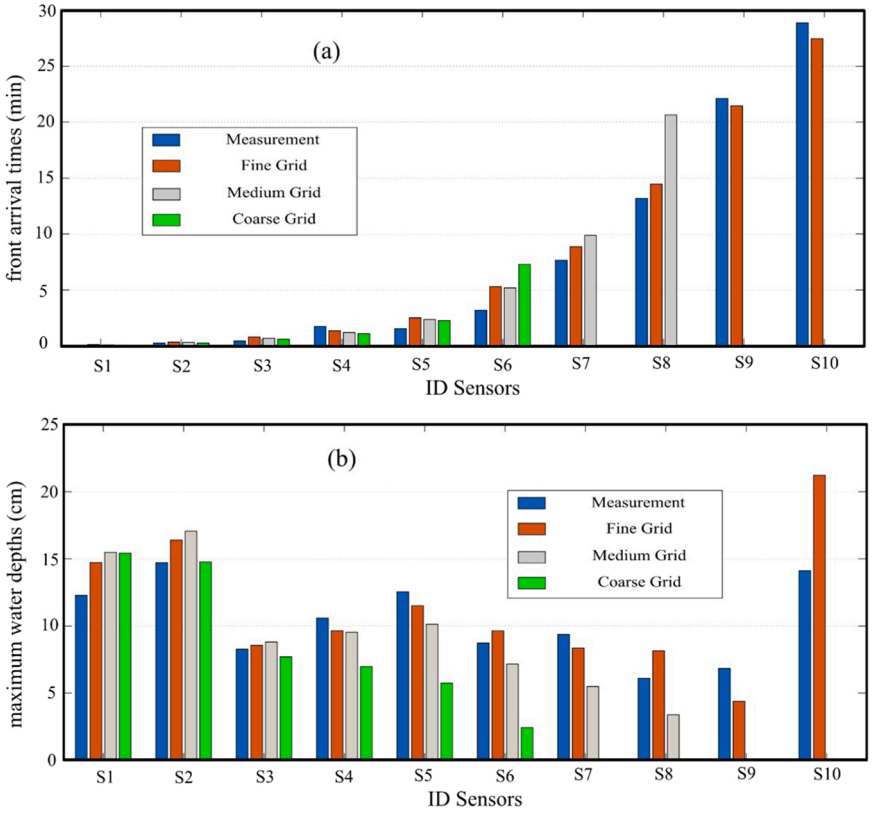

Fig. 8. Grid resolution effects on times of waterfront advance (a) and maximum water depths (b).

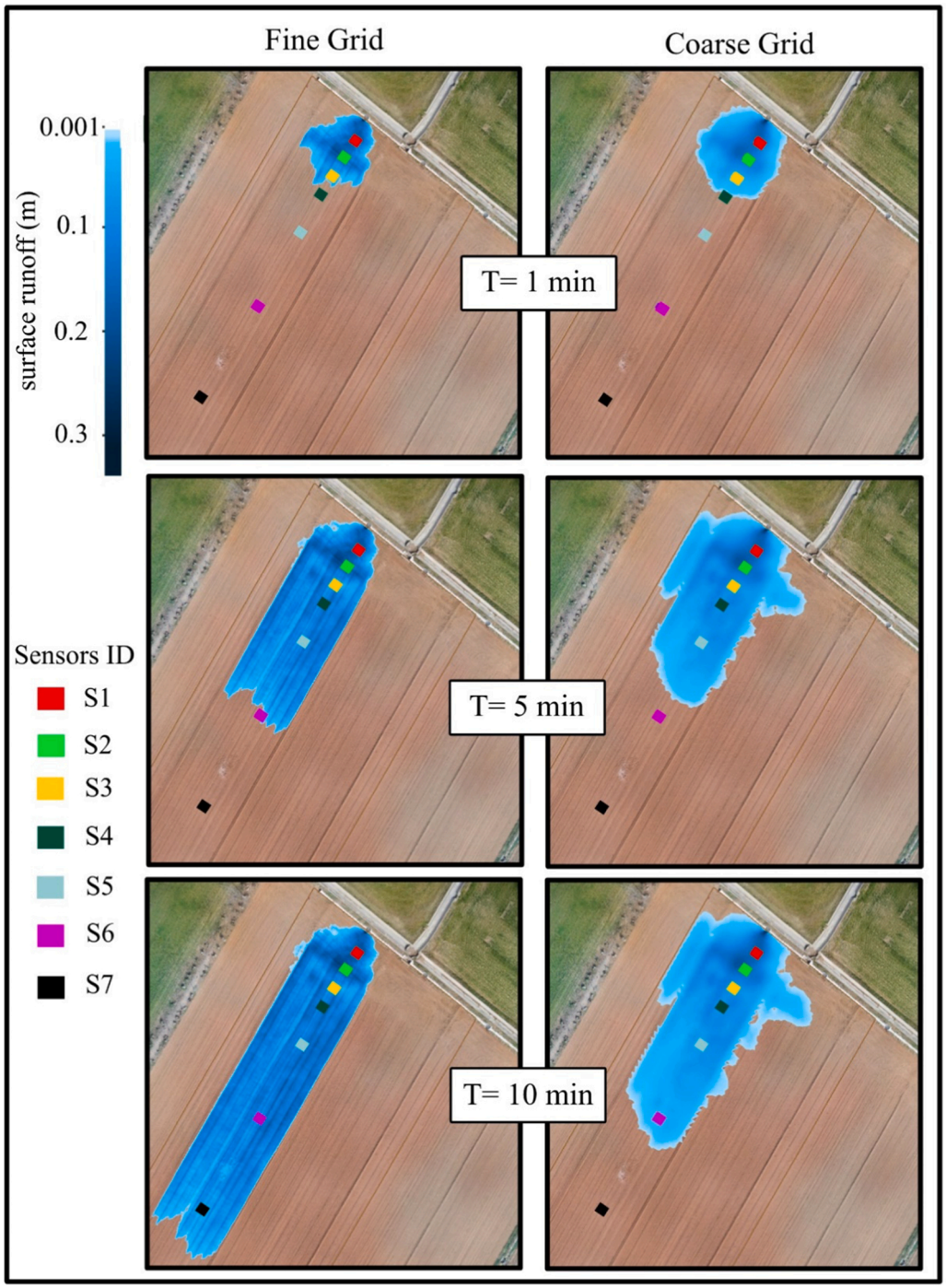

Fig. 9. Influence of grid resolution on surface irrigation dynamics. The coloured boxes represent the positions of the sensors S1, S2 … S10 shown in Fig. 3.

5. Discussion

The RMSE values reported in Table 4 highlighted that grid resolution change from coarse to medium didn't improve model performance too much, while from medium to fine the model performance was improved a lot. Therefore, searching for a critical grid resolution as a trade-off between computational time and model performance, could be interesting. For this reason, three additional computational grids have been generated having resolutions equal to 0.02 m^2, 0.05 m^2 and 0.08 m^2. For comparative purposes, we introduce here the Accuracy Variation Index (AVI) and the Performance Variation Index (PVI) defined as in Eq. (7) and Eq. (8), respectively:

$$AVI = \frac{\text{RMSE(fine grid)}}{\text{RMSE(generic grid)}} \tag{7}$$

$$PVI = 1 - \frac{\text{computational time (generic grid)}}{\text{computational time (fine grid)}} \tag{8}$$

in which RMSE values are related to the timings of waterfront advance. AVI provides information about the accuracy of the solution obtained using a generic grid compared to that obtained with the finest grid. Its value is lower than 1 and approaches to zero as the RMSE of the generic grid deviates with respect to that of the fine grid. PVI gives indication about the computational time saving induced by the use of a generic grid

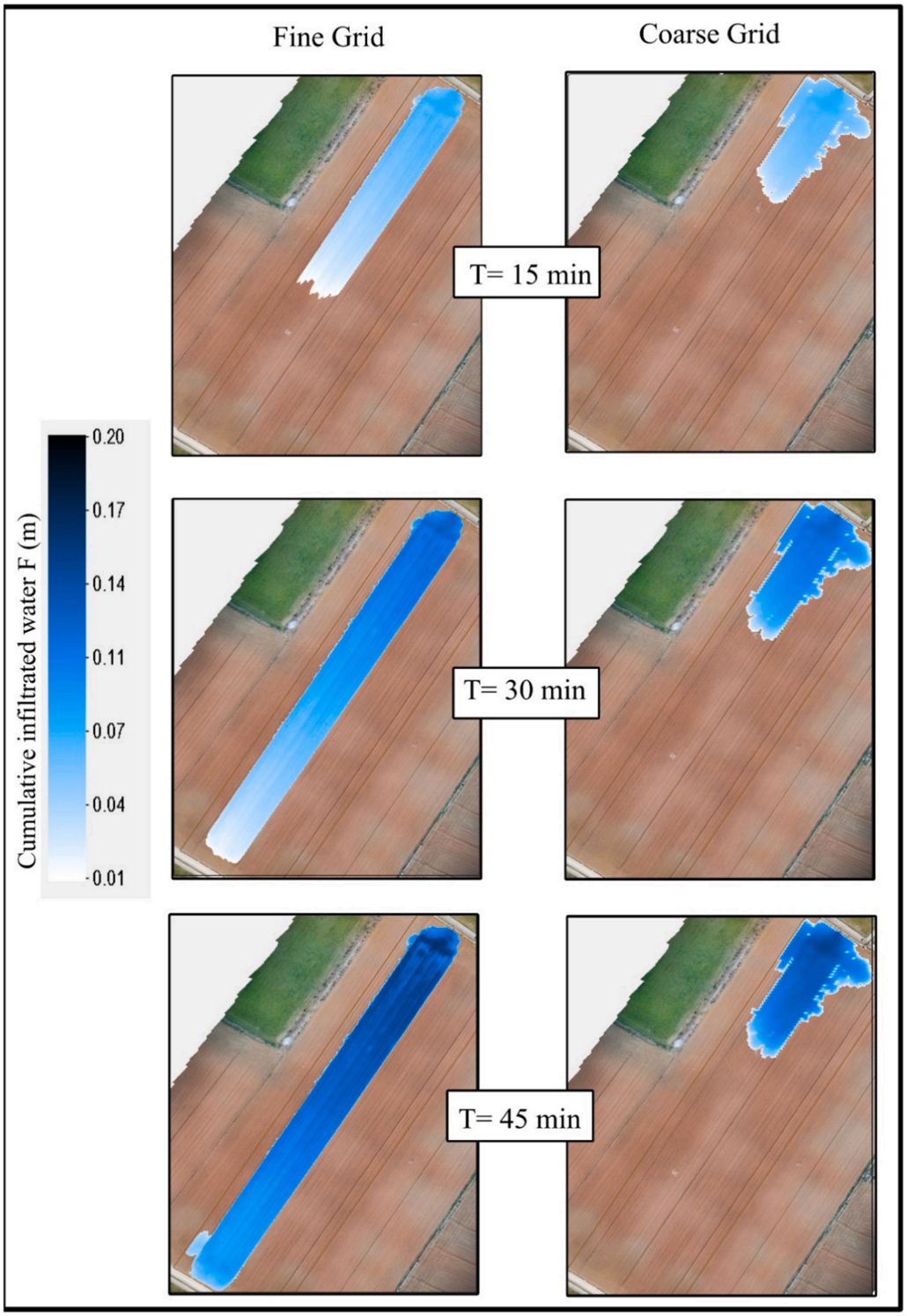

Fig. 10. Influence of grid resolution on cumulative infiltrated water *F*, computed using Eq. (4).

in relation to the finest grid. Therefore, the greater its value the greater is the reduction of the run time. Both AVI and PVI values, expressed as function of the grid resolution ratio GRR defined as the ratio between the resolution of the generic and the finest grids, are reported in Fig. 11.

Fig. 11 highlights the fact that the accuracy of the solution is characterized by a non-linear behavior in which, as expected, AVI decreases as the grid size increases. In particular, doubling the area of the computational element with respect to the finest grid (GRR=2) induces the halving of AVI (~0.5). However, for GRR= 2 the RMSE value is about 2.2 min, so that the overall result may be still considered satisfying. For GRR> 8, AVI reduces of one order of magnitude and the overall accuracy seems to be independent from the GRR value, confirming what has been reported in Table 4. Moreover, the waterfront stopped before the end of the field for GRR values equal to or greater than 8, and this contradicted the observations.

Conversely, the performance in terms of computational times rapidly increases for lower values of GRR whereas no significant benefits can be observed for GRR> 5. In particular, for GRR= 2 the PVI value is

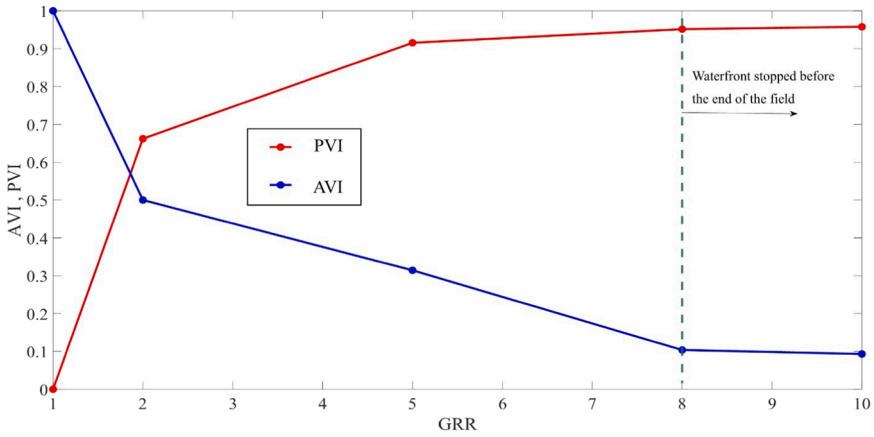

Fig. 11. AVI and PVI values, computed using Eqs. (7) and (8), against the GRR ratio.

approximately 0.65, meaning that doubling the area of the computational cell in respect to the finest grid leads to an important reduction of the computational times. Of course, the PVI values are strictly connected to both the hardware characteristics of the CPU Cluster used in this work and the efficiency of the numerical code, therefore they should be considered carefully just as a gross indication. However, the simulation related to GRR= 2, that is grid resolution equal to 0.02 m^2, seems to be a good balance between accuracy of the results and reduced computational times.

As in any modelling study, model calibration is required where the optimized parameters are not readily observed. In modelling framework of this study, three out of four parameters (K_s, ψ, and n) were slightly adjusted starting from those suggested in literature, whereas the remaining one, $\Delta\theta$, was obtained by combining field measurements of volumetric water content before the irrigation events and literature values of effective porosity. With regard to the set of parameter values that provided the best performances (SIM 8 - Table 3), it is interesting to note that n and K_s fall exactly within the range reported in literature for the type of soil of the experimental field (SIM 1 – Table 3), while ψ is larger (i.e. from 5 cm to 20 cm). This is probably due to the dependence of the water suction head in the GA infiltration process on initial soil moisture conditions (ϑ_i). In fact, Aggelides and Youngs (1978), by investigating the dependence of the GA parameters on the initial water content in draining and wetting states, found that in sandy soils ψ was significantly influenced by the initial soil moisture condition when this latter resulted in less than 0.3 m^3/m^3. They found a linear relationship between ψ and ϑ_i which in case of ϑ_i equal to 0.2 m^3/m^3 (i.e. the initial soil moisture condition registered in our case study), the value of ψ resulted in about 17 cm, very close to the value found in our study. These results demonstrate the reliability of the proposed modelling approach in reproducing surface dynamics also when typical literature observations for calibrating GA and roughness are used.

Concerning the simulation of the infiltration process, additional spatial and temporal measurements of infiltration volumes should be performed for validating the model estimations. However, in the absence of these data, the good representation of the surface phenomenon, while respecting the conservation of the mass, also implies a good representation of the infiltration process. In fact, in Githui et al. (2020) the infiltration volume in time, compared to the numerical results, is obtained as the difference between the total incoming volume and that one observed on the surface. This confirms that performing good measurements of water depth along the longitudinal direction of the field during irrigation events (as carried out in our work), can help to validate the model estimations both in surface water dynamic and infiltration process.

A limitation of the proposed modelling approach is that the spatial and temporal variability of GA model parameters is neglected. Moreover, the use of a constant roughness parameter could influence flow dynamics as well. The effect of these limitations can be observed in Fig. 7 where the simulated water depths are slightly inconsistent with observations especially at the end of the field (point S10), i.e. where the velocities are reduced. In the study of Mailapalli et al. (2008) a methodology for taking into account the spatial and temporal variation of Manning's roughness coefficient under bare and cropped field conditions as well as between the irrigation events was developed. More in detail, Manning's coefficient n varied with the crop growing, water depth, flow velocity and in particular before and after the cut-off time. However, the complexity and the computational effort of the Mailapalli et al. (2008) solution were not accompanied by a significant improvement in the description of surface irrigation dynamics. This further confirms that the IrriSurf2D approach can provide a reliable representation of the dynamics of surface waterings without requiring very high model complexity and computational times.

Concerning the results obtained with grids of different resolutions, Table 4 and Figs. 8–10 demonstrate that the ground microtopography details are needed for an exhaustive representation of surface and subsurface water dynamics in border irrigation. This result corroborates the experimental evidence found by Bai et al. (2011) and Githui et al. (2020). High-resolutions of topographic characteristics of the ground surface are required if a 2D hydrodynamic modelling is used for describing dynamics of surface irrigations especially when water depths onto the field are of the same order of magnitude as ground roughness.

Finally, it may be interesting to highlight the good efficiency of the numerical model used in this work, since it is configured for parallel execution using Message Passing Interface (MPI) directives in order to drastically reduce the computational time. To the author's knowledge, this is the first time in the literature that such an approach is used in the context of surface irrigation.

6. Conclusion

In this work, IrriSurf2D, a new integrated modelling framework based on a combination of high-resolution topographic data, infiltration and surface hydrodynamic modelling is proposed with the aim to obtain detailed simulations of border irrigation events and, ultimately, to improve the management of this widespread irrigation method. More in detail, IrriSurf2D couples the two-dimensional shallow water equation with a semi-physical infiltration model based on the Green-Ampt approach in order to describe the advance phase of the border irrigation. IrriSurf2D fully exploits microtopography information obtained by detailed topographic surveys for simulating the surface water dynamics during irrigations and its parameters can be effectively calibrated using on-field measurements of flowrate, cut-off time, timings of water advance, water depths onto the field and soil moisture. Results obtained

using data collected at an experimental field showed that when using a high-resolution grid to represent the microtopography, IrriSurf2D is able to accurately reproduce both times of water advance and water depths onto the field with parameter values falling within the range of variability indicated in the literature for the specific soil of the experimental field. This increases the possibility to apply the modelling framework with a limited amount of field observations for parameters calibration or even when field measurements are not available. However, the results also show that the grid resolution plays a significant role, with simulation quality significantly deteriorating when applying coarser grids.

The results of this work can be considered relevant in view of the implementation of an operational tool aimed to support strategies for improving the design and management of border irrigation. The next goal is to investigate the effects on irrigation performances (i.e. water saving, distribution uniformity etc.) of different combinations of flow rate, cut-off time/distance, field/strip size and initial moisture conditions. The combined effects of microtopography accuracy and spatial and temporal variability of model parameters will be also further investigated. A key challenge will be to translate the findings obtained through a combination of field experiments and modelling exercises into operational guidelines and best practices leading to a significant increase in border irrigation efficiency.

Declaration of Competing Interest

The authors declare that they have no known competing financial interests or personal relationships that could have appeared to influence the work reported in this paper.

Data Availability

Data will be made available on request.

Acknowledgements

This study was developed in the context of the IrriGate project “Toward a smart and flexible irrigation management in gravity-fed irrigation contexts” funded by Regione Lombardia (PSR 1.2.01; year 2019 – grant no. 201901319885). The authors are grateful to Dr. Paolo Magri, Dr. Chiara Salami and Dr. Antonio Panizza from the Garda Chiese reclamation consortia for their support to the project and during on-field measurements. Prof. Livio Pinto, Dr. Michele Pinto, Dr. Francesco Ioli and Dr. Federico Barbieri of Politecnico di Milano that provided excellent additional technical support in photogrammetric surveys and processing. Lastly, the authors are indebted to the farmer (Mr. Diego Remelli) who made his field available for this study.

References

Aggelides, S., Youngs, E.G., 1978. The dependence of the parameters in the Green and Ampt infiltration equation on the initial water content in draining and wetting states. Water Resour. Res. 14 (5), 857–862. https://doi.org/10.1029/WR014i005p00857.

Akbari, M., Gheysari, M., Mostafazadeh-Fard, B., Shayannejad, M., 2018. Surface irrigation simulation-optimization model based on meta-heuristic algorithms. Agric. Water Manag. 201, 46–57. https://doi.org/10.1016/j.agwat.2018.01.015.

Alavi, S.A., Naseri, A.A., Ritzema, H., van Dam, J., Hellegers, P., 2022. A combined model approach to optimize surface irrigation practice: SWAP and WinSRFR. Agric. Water Manag. 271, 107741 https://doi.org/10.1016/j.agwat.2022.107741.

AnonWMO, 2010. Manual on stream gauging (Vol. I & II). World Meteorological Organization, Geneva, Switzerland, 2010. ⟨https://library.wmo.int/doc_num.php?explnum_id=219⟩.

Anwar, A.A., Ahmad, W., Bhatti, M.T., Ul Haq, Z., 2016. The potential of precision surface irrigation in the indus basin irrigation system. Irrig. Sci. 34 (5), 379–396. https://doi.org/10.1007/s00271-016-0509-5.

Bai, M., Xu, D., Li, Y., Zhang, S., Liu, S.S., 2017. Coupled impact of spatial variability of infiltration and microtopography on basin irrigation performances. Irrig. Sci. 35 (5), 437–449. https://doi.org/10.1007/s00271-017-0550-z.

Bai, M.J., Xu, D., Li, Y.N., Pereira, L.S., 2011. Impacts of spatial variability of basins microtopography on irrigation performance. Irrig. Sci. 29, 359–368. https://doi.org/10.1007/s00271-010-0244-2.

Barbero, G., Costabile, P., Costanzo, C., Ferraro, D., Petaccia, G., 2022. 2D hydrodynamic approach supporting evaluations of hydrological response in small watersheds: implications for lag time estimation. J. Hydrol. 610, 127870 https://doi.org/10.1016/j.jhydrol.2022.127870.

Bautista, E., Clemmens, A.J., Strelkoff, T.S., Schlegel, J., 2009. Modern analysis of surface irrigation systems with WinSRFR. Agric. Water Manag. 96 (7), 1146–1154. https://doi.org/10.1016/j.agwat.2009.03.007.

Bo, C., Zhu, O., Shaohui, Z., 2012. Evaluation of hydraulic process and performance of border irrigation with different regular bottom configurations. J. Ecol. 3 (2), 151–160. https://doi.org/10.5814/j.issn.1674-764x.2012.02.007.

Bradford, S.F., Katopodes, N.D., 2001. Finite volume model for nonlevel basin irrigation. J. Irrig. Drain. Eng. 127 (4) https://doi.org/10.1061/(ASCE)0733-9437(2001)127:4(216).

Brouwer, C., Prins, K., Kay, M., Heibloem, M., 1988. Irrigation water management: irrigation methods. Train. Man. 9 (5), 5–7. ⟨https://www.wec.edu.ye/wp-content/uploads/2015/11/Manual5.pdf⟩.

Brufau, P., García-Navarro, P., Playán, E., Zapata, N., 2002. Numerical modeling of basin irrigation with an upwind scheme. J. Irrig. Drain. Eng. 128 (4), 212–223. https://doi.org/10.1061/(ASCE)0733-9437(2002)128:4(212).

Cea, L., Costabile, P., 2022. Flood risk in urban areas: modelling, management and adaptation to climate change: a review. Hydrology 9 (3), 50. https://doi.org/10.3390/hydrology9030050.

Chari, M.M., Davary, K., Ghahraman, B., Ziaei, A.N., 2019. General equation for advance and recession of water in border irrigation. Irrig. Drain. 68 (3), 476–487. https://doi.org/10.1002/ird.2342. ISO 690.

Chen, B., Ouyang, Z., Sun, Z., Wu, L., Li, F., 2013. Evaluation on the potential of improving border irrigation performance through border dimensions optimization: a case study on the irrigation districts along the Lower Yellow River. Irrig. Sci. 31 (4), 715–728. https://doi.org/10.1007/s00271-012-0338-0.

Clemmens, A.J., 1979. Verification of the zero-inertia model for border irrigation. Trans. ASAE 1979 (6), *22*. https://doi.org/10.13031/2013.35203.

Costabile, P., Costanzo, C., 2021. A 2D-SWEs framework for efficient catchment-scale simulations: hydrodynamic scaling properties of river networks and implications for non-uniform grids generation. J. Hydrol. 599, 126306 https://doi.org/10.1016/j.jhydrol.2021.126306.

Costabile, P., Costanzo, C., De Lorenzo, G., Macchione, F., 2020. Is local flood hazard assessment in urban areas significantly influenced by the physical complexity of the hydrodynamic inundation model? J. Hydrol. 580, 124231 https://doi.org/10.1016/j.jhydrol.2019.124231.

Costabile, P., Costanzo, C., Ferraro, D., Barca, P., 2021. Is HEC-RAS 2D accurate enough for storm-event hazard assessment? Lessons learnt from a benchmarking study based on rain-on-grid modelling. J. Hydrol. 603, 126962 https://doi.org/10.1016/j.jhydrol.2021.126962.

Costabile, P., Costanzo, C., Gandolfi, C., Gangi, F., Masseroni, D., 2022. Effects of DEM depression filling on river drainage patterns and surface runoff generated by 2D rain-on-grid scenarios. Water (Switz.) 14 (7), 997. https://doi.org/10.3390/w14070997.

Fadul, E., Masih, I., De Fraiture, C., Suryadi, F.X., 2020. Irrigation performance under alternative field designs in a spate irrigation system with large field dimensions. Agric. Water Manag. 231, 105989 https://doi.org/10.1016/j.agwat.2019.105989.

Fiedler, F.R., Ramirez, J.A., 2000. A numerical method for simulating discontinuous shallow flow over an infiltrating surface. Int. J. Numer. Methods Fluids 32 (2), 219–239 https://doi.org/10.1002/(SICI)1097-0363(20000130)32:2<219::AID-FLD936>3.0.CO;2-J.

Gagliolo, S., Fagandini, R., Passoni, D., Federici, B., Ferrando, I., Pagliari, D., Pinto, L., Sguerso, D., 2018. Parameter optimization for creating reliable photogrammetric models in emergency scenarios. Appl. Geomat. 10 (4), 501–514. https://doi.org/10.1007/s12518-018-0224-4.

Gandolfi, C., Savi, F., 2000. A mathematical model for the coupled simulation of surface runoff and infiltration. J. Irrig. Drain. Eng. 75 (1), 49–55. https://doi.org/10.1006/jaer.1999.0484.

Gillies, M.H., Smith, R.J., 2015. SISCO: surface irrigation simulation, calibration and optimisation. Irrig. Sci. 33 (5), 339–355. https://doi.org/10.1007/s00271-015-0470-8.

Githui, F., Hussain, A., Morris, M., 2020. Incorporating infiltration in the two-dimensional ANUGA model for surface irrigation simulation. Irrig. Sci. 38 4, 373–387. https://doi.org/10.1007/s00271-020-00679-y.

Green, W., Ampt, G.A., 1911. Studies on soil phyics, part I-the flow of air and water through soils. J. Agric. Sci. 4 (1), 1–24. https://doi.org/10.1017/S0021859600001441.

Kacimov, A.R., Al-Ismaily, S., Al-Maktoumi, A., 2010. Green-ampt one-dimensional infiltration from a ponded surface into a heterogeneous soil. J. Irrig. Drain. Eng. 136 (1), 68–72. https://doi.org/10.1061/(ASCE)IR.1943-4774.0000121.

Khanna, M., Malano, H.M., 2006. Modelling of basin irrigation systems: a review. Agric. Water Manag. 83 (1–2), 87–89. https://doi.org/10.1016/j.agwat.2005.10.003.

Khanna, M., Malano, H.M., Fenton, J.D., Turral, H., 2003. Two-dimensional simulation model for contour basin layouts in southeast australia. II: irregular shape and multiple basins. J. Irrig. Drain. Eng. 129 (5) https://doi.org/10.1061/(ASCE)0733-9437(2003)129:5(317).

Kostiakov, A.N., 1932. On the dynamics of the coefficient of water percolation in soils and on the necessity for studying it from a dynamic point of view for purposes of amelioration. Trans. 6th Comm. Int. Soc. Soil Sci. Part A 17–21. ⟨https://cir.nii.ac.jp/crid/1570572699970385664?lang=en⟩.

Lewis, M.R., 1937. The rate of infiltration of water in irrigation practice. Trans. Am. Geophys. Union. 18, 361–368. https://doi.org/10.1029/TR018i002p00361.

Liu, J., Zhang, S., Dai, W., Xu, D., Bai, M., Li, Y., 2021. Performance comparison between semi-lagrangian and eulerian numerical solutions for two-dimensional surface flows

in basin irrigation. J. Irrig. Drain. Eng. 147 (6) https://doi.org/10.1061/(ASCE)IR.1943-4774.0001560.
Liu, K., Jiao, X., Li, J., An, Y., Guo, W., Salahou, M.K., Sang, H., 2020. Performance of a zero-inertia model for irrigation with rapidly varied inflow discharges. Int. J. Agric. Biol. Eng. 13 (2), 175–181. https://doi.org/10.25165/j.ijabe.20201302.5228.
Mailapalli, D.R., Raghuwanshi, N.S., Singh, R., Schmitz, G.H., Lennartz, F., 2008. Spatial and temporal variation of manning's roughness coefficient in furrow irrigation. J. Irrig. Drain. Eng. 134 (2), 185–192. https://doi.org/10.1061/(ASCE)0733-9437(2008)134:2(185).
Masseroni, D., Ricart, S., De Cartagena, F.R., Monserrat, J., Gonçalves, J.M., De Lima, I., Facchi, A., Sali, G., Gandolfi, C., 2017. Prospects for improving gravity-fed surface irrigation systems in Mediterranean European contexts. Water J. 9 (1), 20. https://doi.org/10.3390/w9010020.
Masseroni, D., Gangi, F., Galli, A., Ceriani, R., De Gaetani, C., Gandolfi, C., 2022. Behind the efficiency of border irrigation: lesson learned in Northern Italy. Agric. Water Manag. 269, 107717 https://doi.org/10.1016/j.agwat.2022.107717.
Mazarei, R., Mohammadi, A.S., Naseri, A.A., Ebrahimian, H., Izadpanah, Z., 2020. Optimization of furrow irrigation performance of sugarcane fields based on inflow and geometric parameters using WinSRFR in Southwest of Iran. Agric. Water Manag. 228, 105899 https://doi.org/10.1016/j.agwat.2019.105899.
Morris, M.R., Hussain, A., Gillies, M.H., O'Halloran, N.J., 2015. Inflow rate and border irrigation performance. Agric. Water Manag. 155, 76–86. https://doi.org/10.1016/j.agwat.2015.03.017.
Naghedifar, S.M., Ziaei, A.N., Playán, E., Zapata, N., Ansari, H., Hasheminia, S.M., 2019. A 2D curvilinear coupled surface–subsurface flow model for simulation of basin/border irrigation: theory, validation and application. Irrig. Sci. 37 (2), 151–168. https://doi.org/10.1007/s00271-018-0609-5.
Padulano, R., Costabile, P., Costanzo, C., Rianna, G., Del Giudice, G., Mercogliano, P., 2021. Using the present to estimate the future: a simplified approach for the quantification of climate change effects on urban flooding by scenario analysis. Hydr. Process. 35 (12), e14436 https://doi.org/10.1002/hyp.14436.
Pagliari, D., Rossi, L., Passoni, D., Pinto, L., De Michele, C., 2017. Avanzi F. Measuring the volume of flushed sediments in a reservoir using multi-temporal images acquired with UAS. Geomat. Nat. Hazards Risk 8 (1), 150–166. https://doi.org/10.1080/19475705.2016.1188423.
Pereira, L.S., Oweis, T., Zairi, A., 2002. Irrigation management under water scarcity. Agric. Water Manag. 57 (3), 175–206. https://doi.org/10.1016/S0378-3774(02)00075-6.
Pereira, L.S., Gonçalves, J.M., Dong, B., Mao, Z., Fang, S.X., 2007. Assessing basin irrigation and scheduling strategies for saving irrigation water and controlling salinity in the upper Yellow River Basin, China. Agric. Water Manag. 93, 109–122. https://doi.org/10.1016/j.agwat.2007.07.004.
Peruzzi, C., Galli, A., Chiaradia, E.A., Masseroni, D., 2021. Evaluating longitudinal dispersion of scalars in rural channels of agro-urban environments. Environ. Fluid Mech. 21, 925–954. https://doi.org/10.1007/s10652-021-09804-7.
Playán, E., Walker, W.R., Merkley, G.P., 1994. Two-dimensional simulation of basin irrigation. I: theory. J. Irrig. Drain. Eng. 120 https://doi.org/10.1061/(ASCE)0733-9437(1994)120:5(837).
Playán, E., Faci, J.M., Serreta, A., 1996. Modeling microtopography in basin irrigation. J. Irrig. Drain. Eng. 122 (6), 837–856. https://doi.org/10.1061/(ASCE)0733-9437(1996)122:6(339).
Rawls, W.J., Brakensiek, D.L., Miller, N., 1983. Green-Ampt infiltration parameters from soils data. J. Hydraul Eng. 109 (1), 62–70. https://doi.org/10.1061/(ASCE)0733-9429(1983)109:1(62).
Salahou, M.K., Jiao, X., Lü, H., 2018. Border irrigation performance with distance-based cut-off. Agric. Water Manag. 201, 27–37. https://doi.org/10.1016/j.agwat.2018.01.014.
Schmitz, G.H., Seus, G.J., 1989. Analytical model of level basin irrigation. J. Irrig. Drain. Eng. 115 (1) https://doi.org/10.1061/(ASCE)0733-9437(1989)115:1(78).
Sharifi, H., Roozbahani, A., Hashemy Shahdany, S.M., 2021. Evaluating the performance of agricultural water distribution systems using FIS, ANN and ANFIS intelligent models. Water Resour. Manag. 35 (6), 1797–1816. https://doi.org/10.1007/s11269-021-02810-w.
Singh, V., Bhallamudi, S.M., 1997. Hydrodynamic modeling of basin irrigation. J. Irrig. Drain. Eng. 123 (6), 407–414. https://doi.org/10.1061/(ASCE)0733-9437(1997)123:6(407).
Smith, R.J., Raine, S.R., Minkevich, J., 2005. Irrigation application efficiency and deep drainage potential under surface irrigated cotton. Agric. Water Manag. 71 (2), 117–130. https://doi.org/10.1016/j.agwat.2004.07.008.
Smith, R.J., Uddin, M.J., Gillies, M.H., 2018. Estimating irrigation duration for high performance furrow irrigation on cracking clay soils. Agric. Water Manag. 206, 78–85. https://doi.org/10.1016/j.agwat.2018.03.014.
Soroush, F., Fenton, J.D., Mostafazadeh-Fard, B., Mousavi, S.F., Abbasi, F., 2013. Simulation of furrow irrigation using the slow-change/slow-flow equation. Agric. Water Manag. 116, 160–174. https://doi.org/10.1016/j.agwat.2012.07.008.
Strelkoff, T., Souza, F., 1984. Modeling effect of depth on furrow infiltration. J. Irrig. Drain. Eng. 110 (4) https://doi.org/10.1061/(ASCE)0733-9437(1984)110:4(375).
Strelkoff, T.S., Tamimi, A.H., Clemmens, A.J., 2003. Two-dimensional basin flow with irregular bottom configuration. J. Irrig. Drain. Eng. 129 (6), 391–401. https://doi.org/10.1061/(ASCE)0733-9437(2003)129:6(391).
Ven Te Chow, 1959. Open-channel Hydraulics. McGraw-Hill, New York, p. 1959. ISBN 978-0-07- 085906-7. ⟨https://heidarpour.iut.ac.ir/sites/heidarpour.iut.ac.ir/files/u32/open-chow.pdf⟩.
Vico, G., Porporato, A., 2011. From Rainfed Agriculture to Stress-Avoidance Irrigation: I. A Generalized Irrigation Scheme with Stochastic Soil Moisture. Adv. Water Resour. 34 (2), 263–271. https://doi.org/10.1016/j.advwatres.2010.11.010.
Walker, W.R., 2003. SIRMOD III- Surface irrigation simulation, evaluation and design. In: Guide and Technical Documentation, 2003. Dept of Biological and Irrigation Engineering, Utah St Univ, Logan, UT, USA. ⟨https://docplayer.net/20847073-Sirmod-iii-surface-irrigation-simulation-evaluation-and-design.html⟩.
Walker, W.R., Humpherys, A.S., 1983. Kinematic-wave furrow irrigation model. J. Irrig. Drain. Eng. 1983 (4), 109. ⟨https://eprints.nwisrl.ars.usda.gov/id/eprint/410/1/518.pdf⟩.
Xu, J., Cai, H., Saddique, Q., Wang, X., Li, L., Ma, C., Lu, Y., 2019. Evaluation and optimization of border irrigation in different irrigation seasons based on temporal variation of infiltration and roughness. Agric. Water Manag. 214, 64–77. https://doi.org/10.1016/j.agwat.2019.01.003.
Zapata, N., Playán, E., 2000. Simulating elevation and infiltration in level-basin irrigation. J. Irrig. Drain. Eng. 126 (2), 78–84. https://doi.org/10.1061/(ASCE)0733-9437(2000)126:2(78).
Zerihun, D., Feyen, J., Reddy, J.M., 1997. Empirical functions for dependent furrow irrigation variables. 1. Methodology and equations. Irrig. Sci. 17 (3) https://doi.org/10.1007/s002710050029.
Zhang, S., Bai, M., Xia, Q., Yu, H., 2017. Efficient simulation of surface water flow in 2D basin irrigation using zero-inertia equations. J. Irrig. Drain. Eng. 143 (1) https://doi.org/10.1061/(ASCE)IR.1943-4774.0001121.